Progress In Electromagnetics Research B, Vol. 93, 67–85, 2021

Effect of Spatial Consistency Parameters on 5G Millimeter Wave Channel Characteristics

Abdelbasset Bedda Zekri[1], Riadh Ajgou[1, *], and El-Hadi Meftah[2]

Abstract—This paper mainly deals with the channel diversity and the effect of spatial consistency parameters for different millimeter wave (mmWave) bands (28, 38, and 73 GHz) according to the channel parameters of the NYUSIM model. Statistical analyses are performed for various spatial consistency scenarios in an urban microcell (UMi) environment. Most of the recent analyses ignored the effect of adjusting the spatial consistency parameters on the 5G mmWave channel characteristics, including path loss (PL), received power, and path loss exponent (PLE). As a result, we have analyzed the effect of each parameter mentioned above for both directional power delay profile (DPDP) and omnidirectional power delay profile (OPDP). Numerical results illustrate how the characteristics of mmWave channel communication can be affected by changing the spatial consistency parameters.

1. INTRODUCTION

Wireless channel modeling has been extensively studied for several millimeter waves (mmWave) frequencies under different scenarios and environmental conditions for 5G networks, thereby making it increasingly important [1]. Spatial consistency scenario is a major issue in the field of statistical analysis of mmWaves channel propagation [2–6]. Overall, the spatial consistency channel model is defined by when the user moves along a given track and produces a correlated and sequential channel impulse response at successive sample points on the track [6]. Therefore, in the context of channel modeling, spatial consistency refers to similar and correlated scattering environments in both large and small scale settings [7]. In general, we can classify channel model scenarios into indoor/outdoor and therefore urban microcells (UMi), macro urban (UMa), and macro rural (RMa) for LOS/NLOS environments [1].

Statistical channel models often use wide variables as well as shadow fading (SF), propagation delay, time groups, and angular spreads, which moreover depend on small-scale parameters such as time excess delay, received power, angle of arrival (AoA), and the angle of departure (AoD) for each multipath component measurement. This work presents the results of several analyses for various environments and spatial variables performed with NYUSIM model [2] and associated simulator (established by the New York university as open-source software) used by the authors in [1, 2, 4]. NYUSIM model exploits the Close In (CI) path loss channel model to perform all channel measurements [2–6].

The primary basis for choosing this model is the use of a purely geometric multiple reflection surface approach to produce spatially correlated and time-varying channel coefficients. These modeling skills generate realistic data when being performed using the Monte Carlo method, thus making this model an excellent measurement-based channel simulator for the design and evaluation of the 5G mmWave bands. Although in the literature, there are many deterministic and statistical channel models which are presented as 5GCM [7], mmMAGIC [8], METIS [9], MiWEBA [10], and 3GPP [11], NYUSIM [2]

Received 17 June 2021, Accepted 26 July 2021, Scheduled 2 August 2021
* Corresponding author: Riadh Ajgou (riadh-ajgou@univ-eloued.dz).
[1] LEVRES Laboratory, Department of Electrical Engineering, University of El Oued, El-Oued 39000, Algeria. [2] Department of Electronics, Faculty of Technology, Hassiba Benbouali University of Chlef, P. O. BOX 78C, Chlef 02180, Algeria.

is still the most suitable model. This model is extended from a static drop-based channel model to a dynamic time-varying channel model that fits well through the natural evolution of NYUSIM and other statistical drop-based models [2].

Given the small number of experiments and studies conducted on spatial consistency analysis, we focus on an in-depth analysis of the effect of different parameters on received power, path loss (PL), and path loss exponent (PLE) for both directional power delay profile (DPDP) and omnidirectional power delay profile (OPDP). Moreover, this study considers spatial consistency [3] and omnidirectional/directional power delay profile (PDP) for the case of a mobile terminal with spatial consistency and a static user terminal (UT) without spatial consistency. The considered diverse parameters are: correlation distance, LOS/NLOS, moving distance, the user's velocity, and user track-type for UMi scenario of the 5G system. This work is arranged as follows. Section 2 introduces some related work on mmWave channel modeling related to spatial consistency analysis. Section 3 presents 5G propagation challenges and PL models. In Section 4, we review the most 5G candidates' mmWave channels 28 GHz, 38 GHz, and 73 GHz for spatial consistency parameters scenarios using the NYUSIM model based on the CI model [4, 5]. NYUSIM performs the small-scale parameter update in the spatial consistency procedure based on multiple surface reflections, and five scenarios are discussed in Section 4. Finally, section 5 provides concluding remarks.

2. RELATED WORK

Along with channel modeling tools (SMRCIM [12] and SIRCIM [13]), statistical channel impulse response models have been developed for multi-path components corresponding to microwave frequencies with respect to temporal and spatial correlation. In particular, these simulators investigated the motion, Doppler propagation, and the phase shift resulting from the multivariate components in a limited zone. Some works focus on spatial consistency analysis; however, they are insufficient since some channel characteristics (PL, PLE, received power) are not studied in detail and in depth, especially regarding spatial consistency parameters [3–6]. Using the NYUSIM channel simulator platform, the authors in [6] studied the spatial modeling properties at 73 GHz frequency but considering only one spatial consistency tuning parameter. In [14], the authors developed a modified PL model for spatial consistency analysis, but without examining the spatial consistency effect on various channel characteristic parameters. The authors in [15] compared a geometry-based spatially consistent channel model with a deterministic ray-tracing model to evaluate the properties of the strongest multipath components as a function of the azimuth/elevation angles of arrival and delay of successive spatial locations in 5G UMi. In [16], the authors proposed a model that improves geometry-based stochastic channel models with spatial consistency by selecting the standardized 3GPP 3-dimensional (3D) channel model. This improved model is characterized by a single parameter called decorrelation distance where simulation was done at low frequencies 2 GHz and 28 GHz.

The main contribution of this paper is to investigate the effect of various spatial consistency parameters on the modeling of 5G mmWave channels. The objective is to study channel characteristics in the 5G mmWave band for typical spatial consistency scenarios: correlation distance LOS/NLOS, moving distance, velocity of the user, and user track type in UMi environment. At each 1 m step, the channel coefficients are updated using a spatial coherence process along the UT track (Linear/Hexagonal) in a local area of the cell, considering a channel portion spitted into diverse channel snapshots. However, the characteristics of millimeter wave dynamics can be the subject of further work.

In general, the received power decreases with distance for the small-scale spatial autocorrelation coefficient [3]. Since the scattering environment is not significantly varied in a local area, the large-scale parameters have a greater correlation distance. In effect, the scattering environment is not significantly varied in a local area.

3. STATISTICAL ANALYSIS OF 5G MILLIMETER WAVE CHANNEL MODELING

A major problem in statistical channel modeling is the consideration of spatial consistency scenario, which results in a time-varying channel impulse response in a local environment. To overcome this problem, a rigorous channel modeling is therefore necessary. In this section, based on NYUSIM model,

we analyze the impact of different spatial consistency parameters as a function of received power, PL and PLE of DPDP and OPDP considering absolute delay and tracking of the user's localization distance on 28, 38, and 73 GHz millimeter wave channels.

Considering a spatial consistency scenario, Figure 1 describes the LOS and NLOS mmWave connection for moving mobile station (MBS) also called user terminal (UT). The base station transfers traffic to the core network under LOS/NLOS communication, where NLOS is caused by edifice obstacles between the transceiver and the core network.

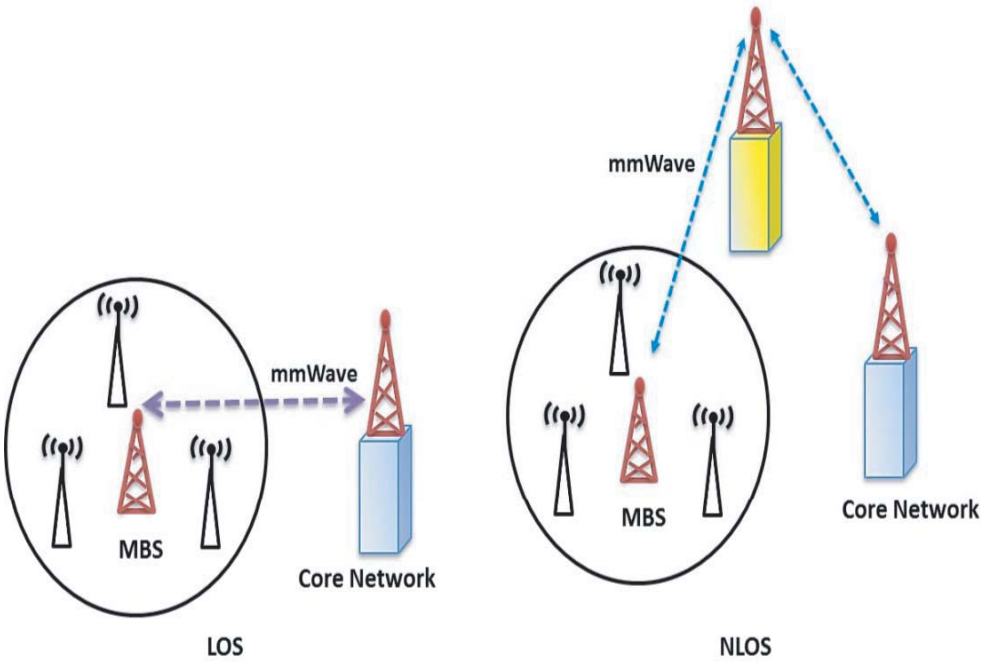

Figure 1. LOS/NLOS scenarios for 5G mmWave networks considering spatial consistency.

3.1. Path Loss

The NYUSIM model adopted in this work uses close-in free space reference distance PL model with a reference distance of 1 m, to which an atmospheric attenuation factor is taken, and this model is given by [3, 6, 14]:

$$PL^{CI}(f,d)\ [\text{dB}] = FSPL(f,1m)\ [\text{dB}] + 10n\log_{10}(d) + AF\,[\text{dB}] + x_{\sigma}^{CI} \tag{1}$$

where f is the carrier frequency [GHz]; $d(d \geq 1m)$ is the distance between TX and RX; n denotes the PLE; AF is defined as the attenuation factor due to atmosphere; x_{σ}^{CI} is described as zero-mean Gaussian random variable (standard deviation σ in dB).

$FSPL(f,1m)$ is the free space PL in the case where the TX/RX distance separation is $1m$ at the carrier frequency f.

$$FSPL(f,1m)\ [\text{dB}] = 10\log_{10}\left(\frac{4\pi f \times 10^{9}}{c}\right) = 32.4\,[\text{dB}] + 20\log_{10}(f) \tag{2}$$

where c is the light speed, of which f is in GHz. We formulate AF by:

$$AF\,[\text{dB}] = \alpha\,[\text{dB/m}] \times d\,[\text{m}] \tag{3}$$

where α is the factor of attenuation in dB/m, which reflects the collective mitigation impact of water vapor fog, dry air, and rain [14], and d is the 3D TX/RX separation distance given in Eq. (1).

3.2. Received Signal Power

The received signal strength depends on TX/RX separation distance d, PL, antenna gains, and the power transmitted. We can estimate the received signal power as [14]:

$$P_R\,[\text{dBm}] = P_T\,[\text{dBm}] + G_T\,[\text{dB}] + G_R\,[\text{dB}] - PL\,(d)\ [\text{dB}] \tag{4}$$

where P_R, P_T, G_T, and G_R are designated respectively as the received signal power, transmitted signal power, and TX/RX antenna gain. In addition, $PL(d)$ indicates the PL average at separation distance d.

3.3. Power Delay Profile (PDP)

To depict omnidirectional power delay profile (OPDP), the omnidirectional channel impulse response is obtained by [17]:

$$h_{omni}\left(t, \vec{\Theta}, \vec{\varphi}\right) = \sum_{n=1}^{N} \sum_{m=1}^{Mn} a_{m,n} e^{j\phi_{m,n}} \times \delta\left(t - \tau_{m,n}\right) \times \delta\left(\vec{\Theta} - \vec{\Theta}_{m,n}\right) \times \delta\left(\vec{\varphi} - \vec{\varphi}_{m,n}\right) \tag{5}$$

where:

t: Propagation time described by absolute form.
$\vec{\Theta} = (\theta, \varphi)TX$: vector features azimuth and elevation angles of departures.
$\vec{\varphi} = (\theta, \varphi)RX$: vector features azimuth and elevation angles of arrivals.
N, M_n: the time clusters (TCs) number and the cluster subpaths number.
$a_{m,n}$: the value of the mth subpaths pertaining to the nth TCs.
$\tau_{m,n}$: the time delays angles.
$\varphi_{m,n}$: the propagation angles.

3.4. Spatial Consistency

Spatial consistency continuously describes the real evolution of the channels along the track of the user terminal (UT) in a determined zone. Toward carrying out spatial consistency, shadow fading (SF) and LOS/NLOS condition maps are established. The correlation distance identifies the notion of "a local zone", which limits the channel portion length (channel portion is about: 10–15 m long).

The channels are well thought-out to be extremely correlated and are updated using a spatial consistency process within a channel portion that can be separated within diverse channel snapshots. We define the updating distance (e.g., 1 m) by the distance between two-channel consecutive snapshots, where the channel coefficients are updated for each 1 m step along the user's terminal track. Figure 2 shows the shadow fade map spatially correlated across the base station (BS) and the user positions. Furthermore, the spatially correlated SF map is created through filtering an independent SF map using an exponential function in Eq. (6). Let us take here: $SF\,[\text{dB}] \sim N(0, 7)$ in a UMi NLOS environment. TX/RX separation distance is 100 m. UT has a hexagonal track with 40 m of moving distance on four portions of 10 m.

Figure 3 shows the UT track in the SF map in which the UT moves clockwise in a partial hexagonal track. Here we consider that the displacement is 40 m, and the length of each side of the hexagon is 10 m. Moreover, the spatially correlated SF and LOS/NLOS condition values are created in the same form.

In terms of SF, a 2-dimensional (2D) grid map is created to hold the spatially correlated SF gains in the simulated zone. The SF is a random variable that follows a log-normal distribution with zero mean and σ standard deviation as described in Eq. (1). At each grid, the map of SF is initialized by assigning independent and identically distributed random variables (i.i.d) fitting normal distribution. An exponential 2-D filter is used with the map, and it is formulated by [18]:

$$h\,(x, y) = \exp\left(-\frac{\sqrt{x^2 + y^2}}{d_{co}}\right) \tag{6}$$

where:

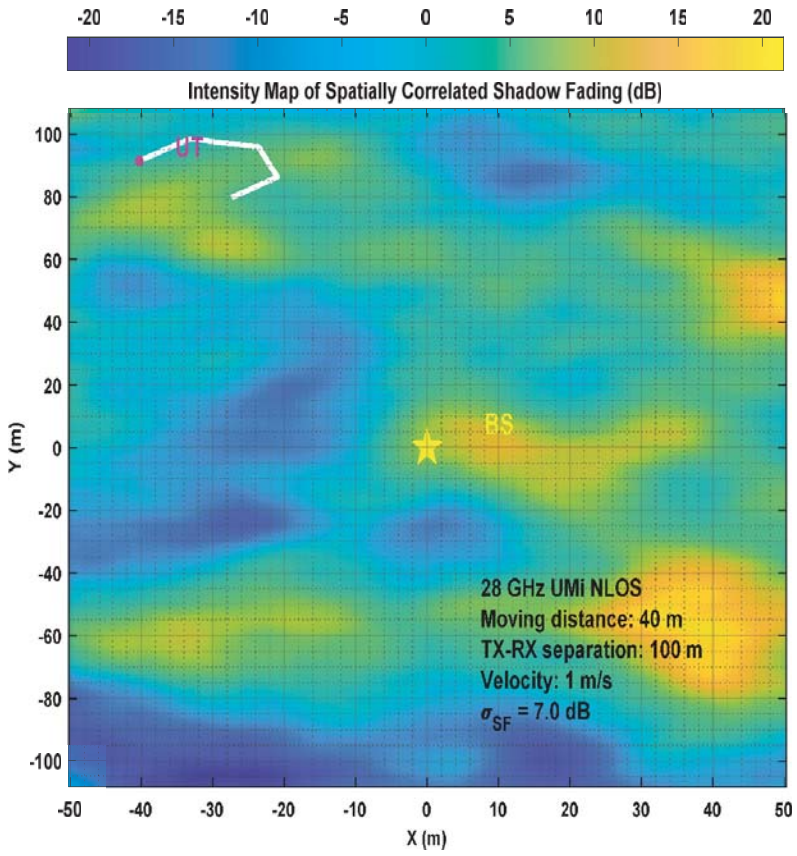

Figure 2. Spatial correlated Shadow Fading Map.

x and y: represent the coordinates of UT with respect to the center of the filter.
$\sqrt{x^2+y^2}$: represents the distance of the filter.
d_{co}: is the correlation distance of SF.

It is worth noting that the LOS/NLOS condition is significant in estimating the performance of wireless communication systems, especially at mmWave frequencies. These conditions define the PLE and shadow fade deviation, while the user's movements between the LOS and NLOS conditions result in a dramatic change in received signal power. Usually, when a UT moves in a local zone, LOS/NLOS condition is the same inside the correlation distance of LOS/NLOS.

By generating a spatially correlated LOS/NLOS condition map, a UT will encounter the same visibility conditions in a local area. Within each channel portion, the visibility condition is kept constant, indicating that the large-scale parameters are spatially consistent. As soon as a UT moves from one channel portion to the next channel portion and its visibility state is changed according to the position of the UT in the map, different parameter values for LOS or NLOS are used to initialize the channel coefficients for the new channel portion. This implies that the LOS/NLOS shift can be applied to the spatially correlated map.

The LOS probability model $\Pr_{LOS}(d)$ used in NYUSIM for 5G UMi scenario is given by [3]:

$$\Pr_{LOS}(d) = \left(\min\left(d_1/d, 1\right)\left(1 - \exp\left(-d/d_2\right)\right) + \exp\left(-d/d_2\right)\right)^2 \tag{7}$$

where d is the 2D Euclidean distance between BS and UT and $(d_1, d_2) = (22\,\text{m}, 100\,\text{m})$.

Figure 4 shows a spatially correlated LOS and NLOS environment map in UMi scenario using the LOS probability in Eq. (7). In addition, the "white zone" represents LOS condition while the "black zone" represents NLOS condition. The size of a UMi cell for mmWave communication systems is typically 200 m [3]. So, the simulated zone is fixed to $200\,\text{m} \times 100\,\text{m}$. The correlation distance is 10 m. The granularity of the map is 1 m. The heights of the BS and UT are 10 m and 1.50 m, respectively.

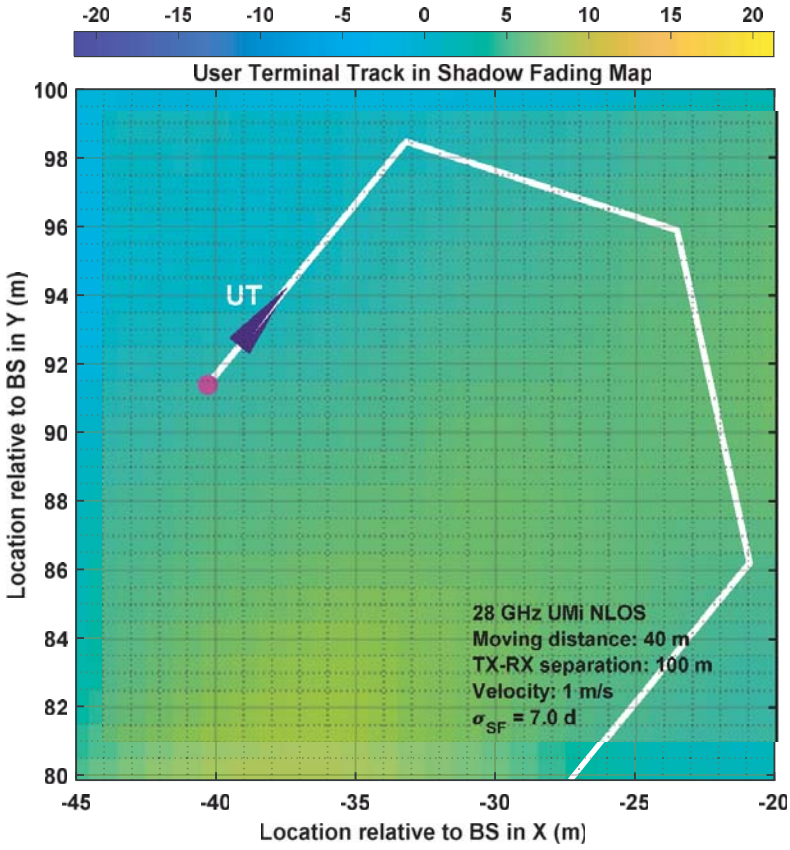

Figure 3. User Terminal track in SF map.

The LOS and NLOS conditions change can affect the UT's track depending on the UT's location on the map.

In line with the NYUSIM channel model [2, 3], the authors of [18] proposed an efficient and dynamic extension for spatial consistency using a modified flowchart-described scheme, which made it possible to achieve spatial consistency and extend a static and drop-based channel model to a dynamic and time-variant one. Figure 5 describes the procedure for generating the spatial coherence parameters using the NYUSIM platform [18]. The new NYUSIM platform aims to update channel coefficients in an iterative way along the UT trajectory. The main steps in the modified flowchart are illustrated as follows [18]:

• Set TX-RX separation distance, UT's velocity, and direction: The update UT distance is less than 1 m so that small changes can be captured compared to the correlation distance of 15 m from large-scale settings. The period to be updated is 0.25 s when the UT speed is 1 m/s [18].

• Assign propagation conditions to spatial correlation (LOS and NLOS): It is obvious that a moving user terminal can take various LOS/NLOS in a selected zone, where the propagation environments at several situations are correlated. Thus, NYUSIM model took into account correlation parameters. The model followed a process similar to that illustrated in [19] by generating the large-scale correlation parameters based on a spatial filter to independent exponential random values.

• Calculate the path loss of time-variant: The path loss is carried out from the UT updated position in each update. Otherwise, the usual variation SF is judged as constant and varied at the propagation condition (LOS and NLOS) deviation.

• Produce time-variant cluster and sub-path excess delays: Initially NYUSIM generates the initial sub-path with cluster delays, where UT is at the start of a half hexagon direction. The excess time delays is updated based on speed, direction, and the time varying AOA/AOD when the UT progresses along the path.

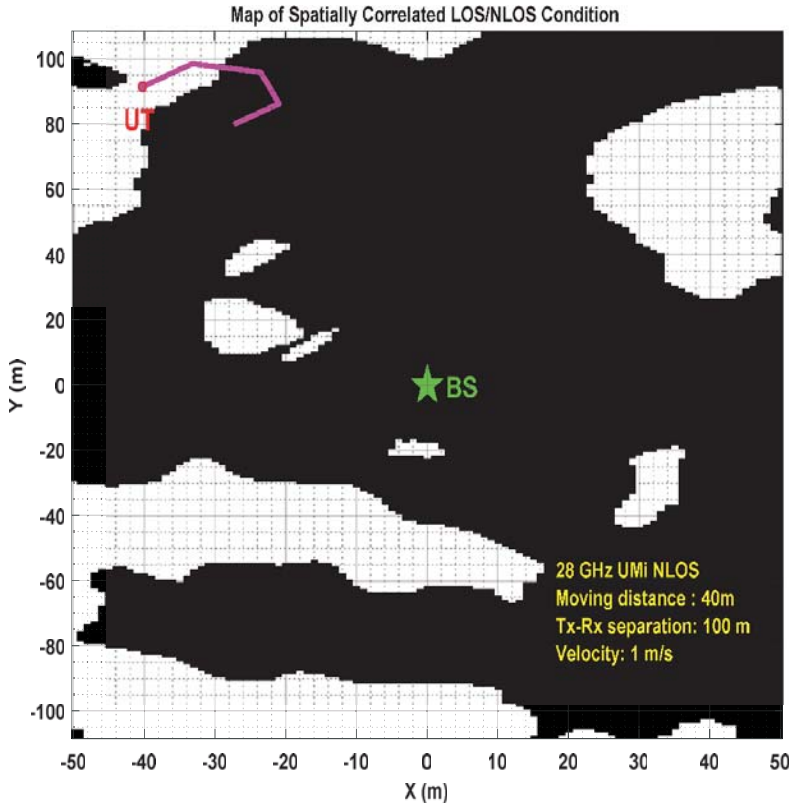

Figure 4. Spatial correlated LOS/NLOS condition map.

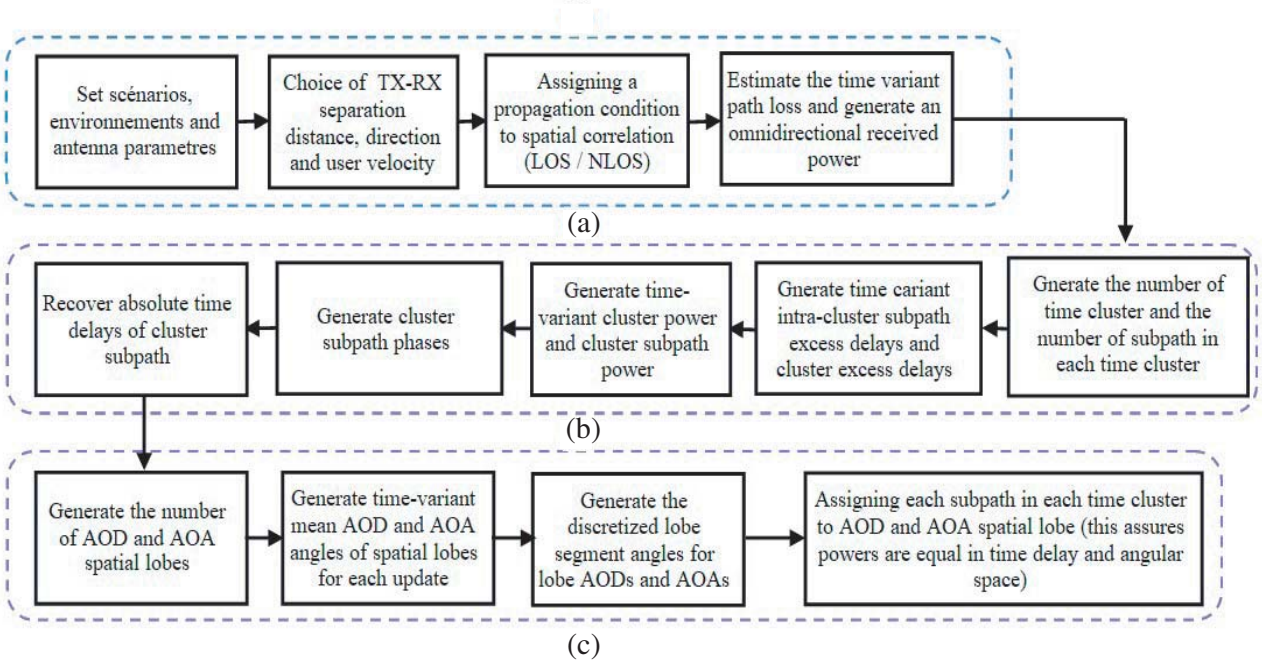

Figure 5. Process for generating spatially consistent channel coefficients. (a) General parameters. (b) Time cluster parameters. (c) Spatial lobe parameters [18].

• Produce time-variant cluster powers and sub-path powers: Clearly, the entire expected power to be captured as well varies due to the time-varying path loss. In addition, the power of each sub-path of each cluster must be allocated during the update in a correlated and continuous manner. The two key parameters in this step are the shadow factors (SFs) for a cluster and for a sub-path. An exponential spatial filter similar to the one adopted to guarantee the probability of correlated LOS is used to build the SFs correlated.

• Produce time-variant sub-path AODs and AOAs: One of the fundamental principles of spatial consistency implementation is to reduce the computational complexity. In fact, spatial consistency algorithms mainly suffer from a high computational complexity. Thus, the extension NYUSIM proposed by authors in [18] related to spatial consistency considers a linear approximation of angles that is introduced before in [20].

The previous steps cited above allowed generating the appropriate statistics for powers, delays, and excessive angles to introduce spatial consistency within NYUSIM model. The use of the new platform showed that the generated channel impulse responses evolved smoothly along the UT track, which confirmed the physical expectation [18]. In this work all the results (Figures and Tables) will be carried out using the NYUSIM model proposed in [18].

4. SIMULATION SCENARIOS AND ANALYSIS OF RESULTS

In this section, we compare some candidate mmWave channels, namely 28 GHz, 38 GHz, and 73 GHz, for various spatial consistency scenarios using the NYUSIM model. Using the well-known NYUSIM platform, we were able to create realistic changes in the temporal and spatial characteristics of broadband channel impulse responses for a mobile terminal. For this purpose, five scenarios are developed based on the properties of the spatial consistency channels (LOS/NLOS correlation distance, moving distance, user's terminal velocity, user's track type). We followed the process to generate spatially consistent channel coefficients as described in Figure 5.

4.1. Correlation Distance LOS/NLOS Scenarios

In the first scenario, a simulation was performed by applying the parameters summarized in Table 1, in which we considered three values (10 m, 15 m, and 20 m) of the LOS/NLOS correlation distance for all studied channels. Table 2 summarizes the directional and omnidirectional power delay statistics at 28, 38, and 73 GHz for correlation distance LOS and NLOS environments. In addition, Figures 6–11

Table 1. Spatial consistency parameters in correlation distance LOS/NLOS scenarios.

Channel Parameters		**Antenna Parameters**	
RF Frequency	28/38/73 GHz	**TX/RX Array Type**	ULA/ULA
RF BW MHz	800	**Num TX/RX Elements**	1/1
Scenario	UMi	**TX/RX Antenna Elements Spacing**	0.5λ/0.5λ
Environment	LOS/NLOS	**TX Azimuth/Elevation HPBW**	10°/10°
T-R Separation (m)	100	**RX Azimuth/Elevation HPBW**	10°/10°
TX Power (dBm)	30	**Spatial consistency Parameters**	
Num RX	1	**Moving distance (m)**	40
Press (mbar)	1013	**Correlation distance LOS/NLOS (m)**	10/15/20
Hum %	50	**Update distance (m)**	1
Temp. C°	20	**Velocity (m/s)**	1
Pol	Co-Pol	**Track type**	Linear
D Foliage (m)	0	**Moving direction (°)**	45°
Rain rate mm/hr	0		

Table 2. Directional and omnidirectional power delay statistics for correlation distance LOS/NLOS scenarios.

Freq Channel [GHz]	Scenario	Correlation distance (m)	Directional Power Delay Profile				Omnidirectional Power Delay Profile			
			RMS DS (ns)	Received Power [dBm]	PL [dB]	PLE	RMS DS (ns)	Received Power [dBm]	PL [dB]	PLE
28	LOS	10	28.98	−57.15	136.51	3.56	22.89	−64.27	94.27	1.56
	LOS	15	25.3	−57.83	137.05	3.95	22.68	−69.01	99.01	1.96
	LOS	20	33.07	−48.82	128.03	3.84	15.08	−68.73	98.73	2.15
	NLOS	10	129.08	−88.84	167.55	5.87	29.52	−84.06	104.06	2.91
	NLOS	15	45.67	−66.06	145.27	4.25	49.53	−91.01	121.01	3.02
	NLOS	20	194.02	−95.57	174.78	5.31	13.7	−102.45	132.45	3.32
38	LOS	10	21.61	−53.37	132.58	3.42	18.65	−97.2	127.2	2.25
	LOS	15	8.48	−50	129.21	3.41	14.41	−71.09	101.09	1.93
	LOS	20	16.58	−56.48	135.69	3.35	22.2	−83.75	113.75	2.32
	NLOS	10	56.8	−69.22	148.43	4.21	24.39	−107.16	137.16	3.65
	NLOS	15	16.76	−75.18	154.39	4.53	11.67	−101.38	131.38	3.38
	NLOS	20	28.05	−57.29	136.5	4.01	43.16	−91.44	121.44	3.18
73	LOS	10	4.3	−52.75	131.96	3.26	17.23	−78.03	108.03	2
	LOS	15	22.02	−57.48	136.69	3.16	11	−80.67	110.67	1.93
	LOS	20	24.39	−46.32	125.53	2.62	18.22	−81.48	111.48	1.96
	NLOS	10	75.23	−90.27	169.48	4.74	35.11	−112.5	142.5	3.46
	NLOS	15	95.43	−86.5	165.71	4.94	59.66	−99.22	129.22	3.06
	NLOS	20	127.79	−99.31	178.53	5.67	16.66	−106.16	136.16	3.46

present the PL, received power, and PLE of both DPDP and OPDP in LOS /NLOS environment for correlation distance LOS/NLOS scenarios.

In the case of the directional power delay profile (DPDP) with LOS scenario, the change in correlation distance has a greater impact on the 73 GHz channel in terms of PL, received power, and PLE, while the impact is very limited on the 28 GHz and 38 GHz channels. For the omnidirectional power delay profile (OPDP) with LOS scenario, this impact is more significant on the 38 GHz channel in PL, received power, however, in terms of PLE the 28 GHz channel is more affected, on the other hand the 38 GHz and 73 GHz channels show the same impact. Finally, for DPDP and OPDP with NLOS, this impact is more significant on the 28 GHz channel.

4.2. Moving Distance Scenarios

For LOS and NLOS environments, with the parameters listed in Table 3, we performed a simulation considering three values (40 m, 50 m, and 60 m) of the moving distance for all studied channels. Table 4 summarizes the results of the directional and omnidirectional Power Delay statistics at 28, 38, and 73 GHz for moving scenario. Figures 12–17 illustrate the PL, received power, and PLE of both DPDP and OPDP in LOS /NLOS environment for moving distance scenarios. Similarly, the effect of the moving distance yields results analogous to those of varying the correlation distance, for both DPDP and OPDP with LOS and NLOS.

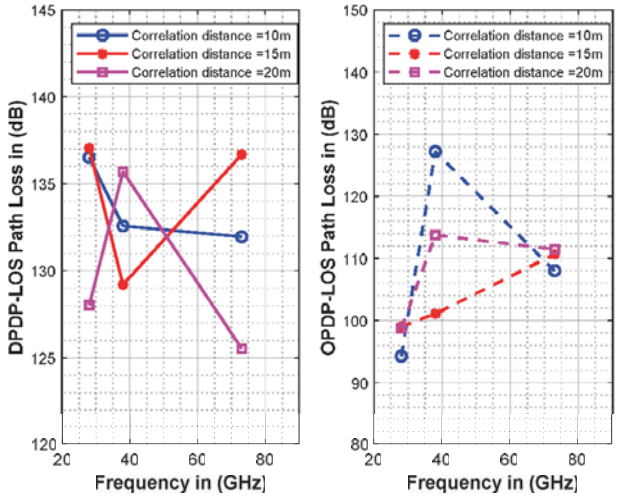

Figure 6. Path loss for DPDP and OPDP LOS on correlation distance LOS/NLOS scenarios.

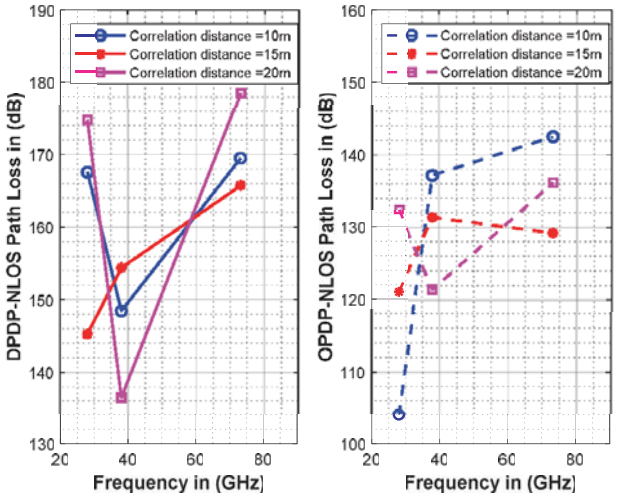

Figure 7. Path loss for DPDP and OPDP NLOS on correlation distance LOS/NLOS scenarios.

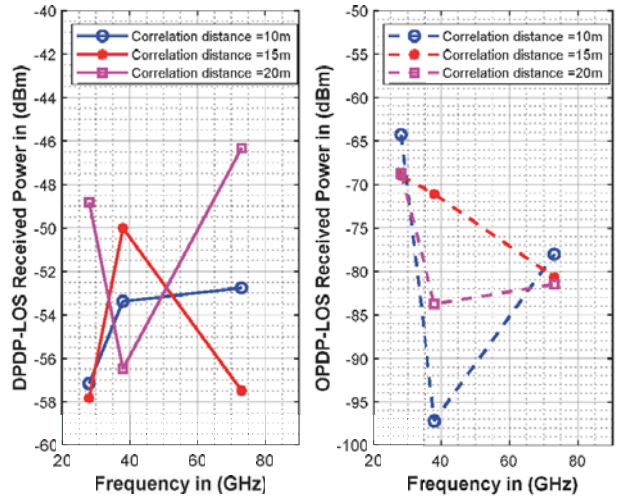

Figure 8. Received Power for DPDP and OPDP LOS on correlation distance LOS/NLOS scenarios.

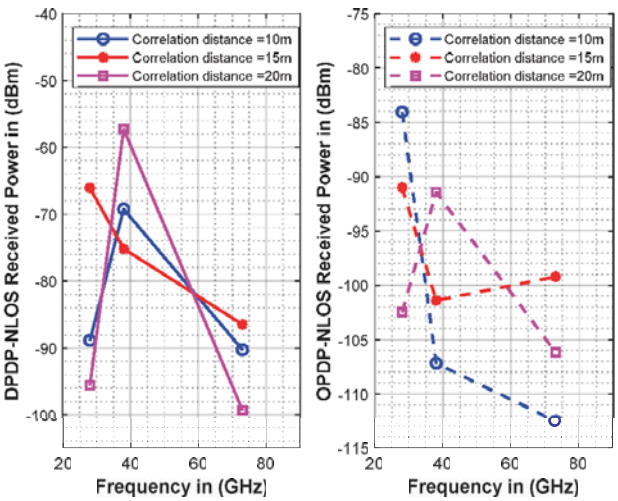

Figure 9. Received Power for DPDP and OPDP NLOS on correlation distance LOS/NLOS scenarios.

4.3. Velocity Scenarios

In this scenario, we performed a simulation with the parameters summarized in Table 5 where we considered three values (1 m/s, 2 m/s, and 5 m/s) of the user's velocity for all studied channels in both LOS and NLOS environments.

Table 6 summarizes the results of the OPDP and DPDP statistics at 28, 38, and 73 GHz for velocity scenario. Figures 18–23 present the PL, received power, and PLE of both DPDP and OPDP within LOS/NLOS environment for velocity scenarios. Based on these figures, regarding the DPDP and OPDP scenario with LOS, the impact of the velocity variation on the PL and PLE received power is more significant on the 38 GHz channel, while this impact is very low on the 28 GHz and 73 GHz channels.

Furthermore, for the DPDP scenario with NLOS, the velocity variation has a stronger impact on the 38 GHz channel in terms of path loss, received power, and path loss exponent, although this impact

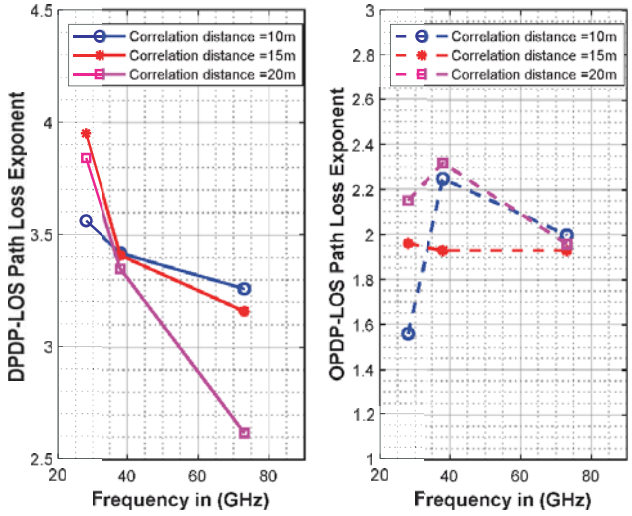

Figure 10. Path Loss Exponent for DPDP and OPDP LOS on correlation distance LOS/NLOS scenarios.

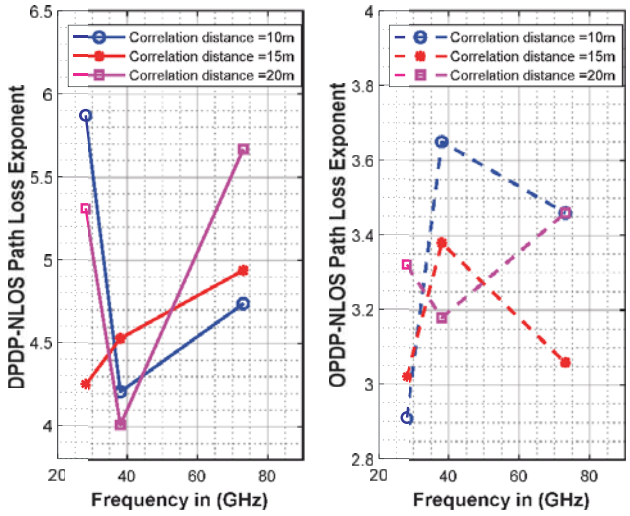

Figure 11. Path loss Exponent for DPDP and OPDP NLOS on correlation distance LOS/NLOS scenarios.

Table 3. Spatial consistency parameters used within moving distance scenarios.

Channel Parameters		**Antenna Parameters**	
RF Frequency	28/38/73 GHz	**TX/RX Array Type**	ULA/ULA
RF BW MHz	800	**Num TX/RX Elements**	1/1
Scenario	UMi	**TX/RX Antenna Elements Spacing**	$0.5\lambda/0.5\lambda$
Environment	LOS/NLOS	**TX Azimuth/Elevation HPBW**	10°/10°
T-R Separation (m)	100	**RX Azimuth/Elevation HPBW**	10°/10°
TX Power (dBm)	30	**Spatial consistency Parameters**	
Num RX	1	**Moving distance (m)**	40/50/60
Press (mbar)	1013	**Correlation distance LOS/NLOS (m)**	10
Hum %	50	**Update distance (m)**	1
Temp. C°	20	**Velocity (m/s)**	1
Pol	Co-Pol	**Track type**	Linear
D Foliage (m)	0	**Moving direction (°)**	45°
Rain rate mm/hr	0		

is roughly the same on the 28 GHz and 38 GHz channels. Finally, for OPDP with NLOS, the impact is more significant on 28 GHz and 73 GHz channels in terms of PL, received power, but in terms of PLE, it is more significant on 38 GHz and 73 GHz channels.

4.4. User Track Type Scenarios

In the last set of simulations, we investigated the impact of changing the user track type on the spatial consistency channels properties. The parameters used in simulations are summarized in Table 7, where we considered two types of user track (Linear/Hexagonal) and for all the channels studied in both LOS

Table 4. Results obtained from directional and omnidirectional power delay statistics for moving distance scenarios.

Freq Channel [GHz]	Scenario	Moving distance (m)	Directional Power Delay Profile				Omnidirectional Power Delay Profile			
			RMS DS (ns)	Received Power [dBm]	PL [dB]	PLE	RMS DS (ns)	Received Power [dBm]	PL [dB]	PLE
28	LOS	40	30.23	−59.12	138.33	3.61	26.72	−76.62	106.62	2.12
	LOS	50	19.83	−56.33	135.54	3.48	9.09	−69.18	99.18	1.77
	LOS	60	24.26	−56.26	135.47	3.56	24.02	−77.37	107.37	2.21
	NLOS	40	40.34	−74.93	154.15	4.92	46.79	−77.22	107.22	2.43
	NLOS	50	35.25	−78.57	157.78	4.46	15.04	−97.14	127.14	3.04
	NLOS	60	69.84	−69.64	148.85	4.68	41.76	−92.57	122.57	3.28
38	LOS	40	23.96	−57.09	136.3	3.66	18.55	−67.2	97.2	1.68
	LOS	50	0.35	−41.98	121.19	2.66	5.6	−75.47	105.47	1.93
	LOS	60	24.53	−54.04	135.25	3.88	23.85	−69.99	99.99	2.01
	NLOS	40	75.97	−77.11	156.32	5.1	49.15	−85.64	115.64	2.88
	NLOS	50	70.87	−70.94	150.15	4.87	16.13	−77.12	107.12	2.43
	NLOS	60	109.79	−84.64	163.85	4.67	26.79	−90.3	120.3	2.63
73	LOS	40	25.36	−56.37	135.58	3.1	22.14	−89.48	119.48	2.34
	LOS	50	24.21	−57.8	137	3.31	12	−80.7	110.7	2.01
	LOS	60	56.54	−74.05	153.26	4.6	15.04	−73.24	103.24	1.84
	NLOS	40	39.95	−77.94	157.15	4.26	14.95	−102.2	122.2	3.05
	NLOS	50	239.2	−96.52	175.73	4.98	19.16	−114.86	144.86	3.46
	NLOS	60	106.79	−89.04	168.25	4.51	34.22	−104.06	134.06	2.95

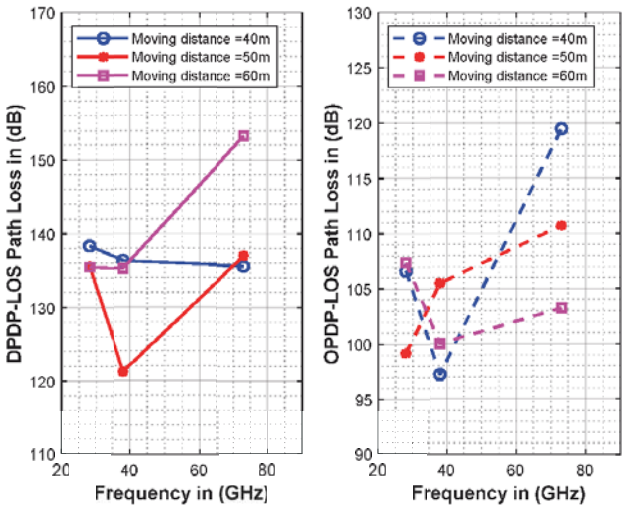

Figure 12. Path loss for DPDP and OPDP LOS on moving distance scenarios.

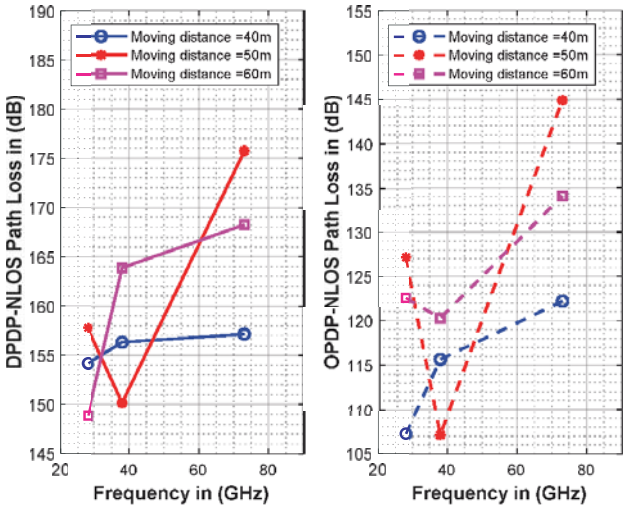

Figure 13. Path loss for DPDP and OPDP NLOS on moving distance scenarios.

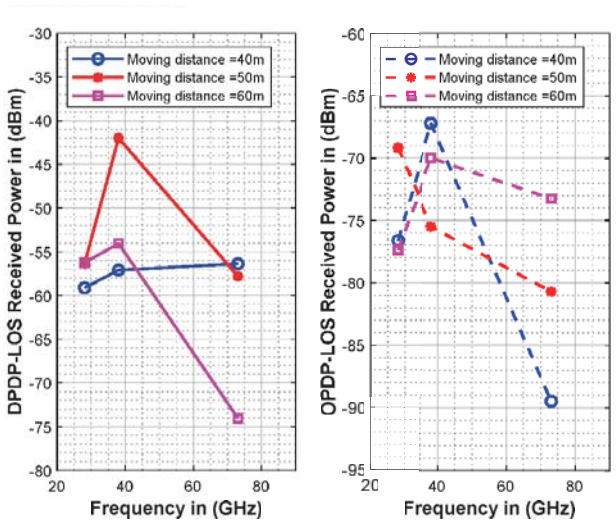

Figure 14. Received Power for DPDP and OPDP LOS on moving distance scenarios.

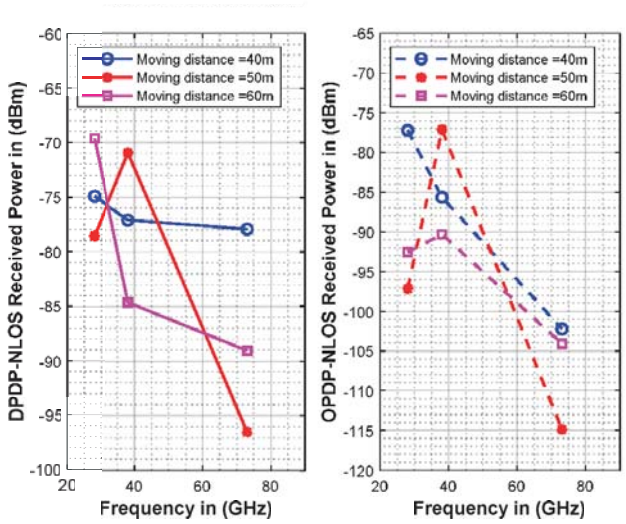

Figure 15. Received Power for DPDP and OPDP NLOS on moving distance scenarios.

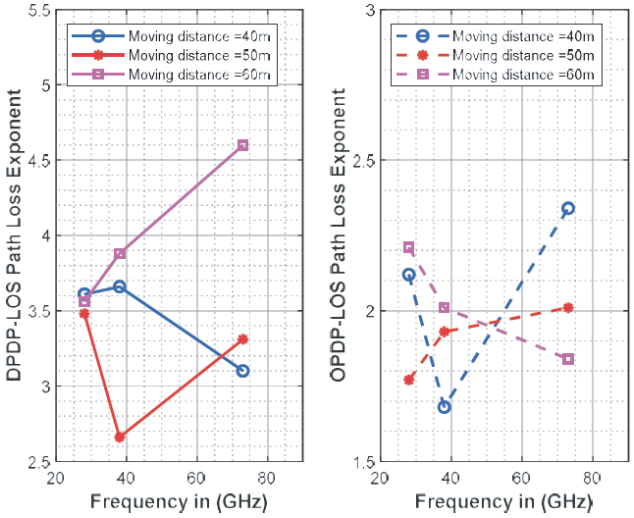

Figure 16. Path Loss Exponent for DPDP and OPDP LOS on moving distance scenarios.

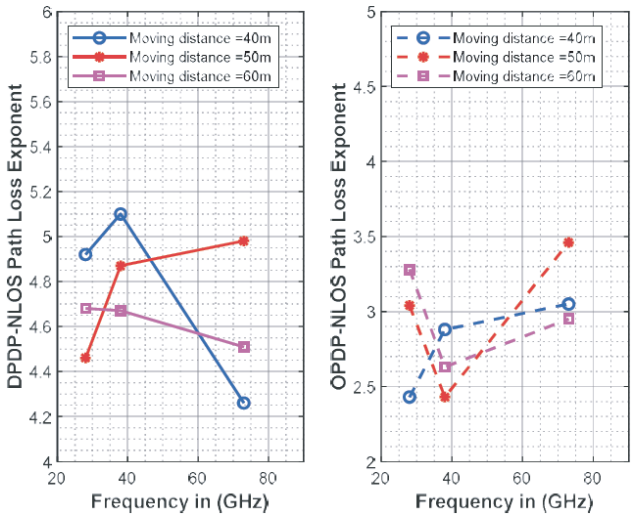

Figure 17. Path Loss Exponent for DPDP and OPDP NLOS on moving distance scenarios.

and NLOS environments.

Table 8 summarizes the results of the DPDP and OPDP statistics at 28, 38, and 73 GHz for the user track type scenario. Figures 24–29 illustrate the PL, received power, and PLE of both DPDP and OPDP in LOS/NLOS environment for the user track type scenarios. As illustrated in these figures, for the DPDP and OPDP using LOS scenarios, the impact of switching channel user type is more significant on the 38 GHz channel with respect to both PL and received power; however in terms of PLE, the impact is more significant on the 28 GHz and 38 GHz channels, whilst on the 73 GHz channel there is very limited impact.

Also, for the DPDP scenario with NLOS, the switch in the user channel type has a more significant impact on the 38 GHz channel with respect to PL, received power and PLE; however, there is an insignificant impact on the 28 GHz channel. Lastly, for OPDP with NLOS, the impact is more significant on the 73 GHz against of PL, received power, and path PLE, but the impact is insignificant on 28 GHz

Table 5. Spatial consistency settings used for the case of user terminal velocity scenarios.

Channel Parameters		Antenna Parameters	
RF Frequency	28/38/73 GHz	**TX/RX Array Type**	ULA/ULA
RF BW MHz	800	**Num TX/RX Elements**	1/1
Scenario	UMi	**TX/RX Antenna Elements Spacing**	0.5λ/0.5λ
Environment	LOS/NLOS	**TX Azimuth/Elevation HPBW**	10°/10°
T-R Separation (m)	100	**RX Azimuth/Elevation HPBW**	10°/10°
TX Power (dBm)	30	**Spatial consistency Parameters**	
Num RX	1	**Moving distance (m)**	40
Press (mbar)	1013	**Correlation distance LOS/NLOS (m)**	10
Hum %	50	**Update distance (m)**	1
Temp. C°	20	**Velocity (m/s)**	1/2/5
Pol	Co-Pol	**Track type**	Linear
D Foliage (m)	0	**Moving direction (°)**	45°
Rain rate mm/hr	0		

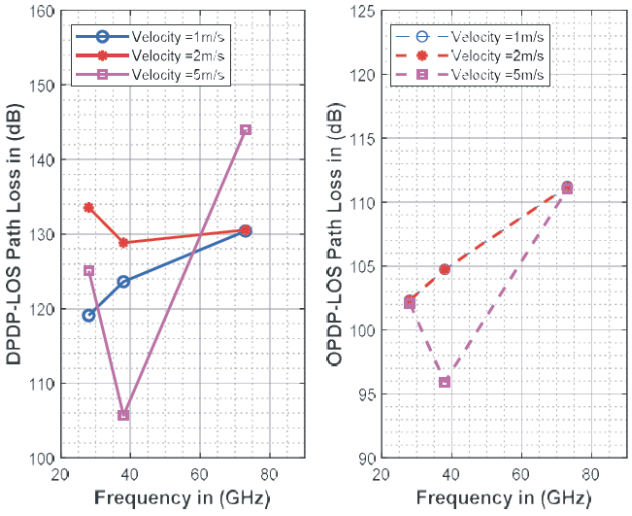

Figure 18. Path loss for DPDP and OPDP LOS on velocity of user terminal scenarios.

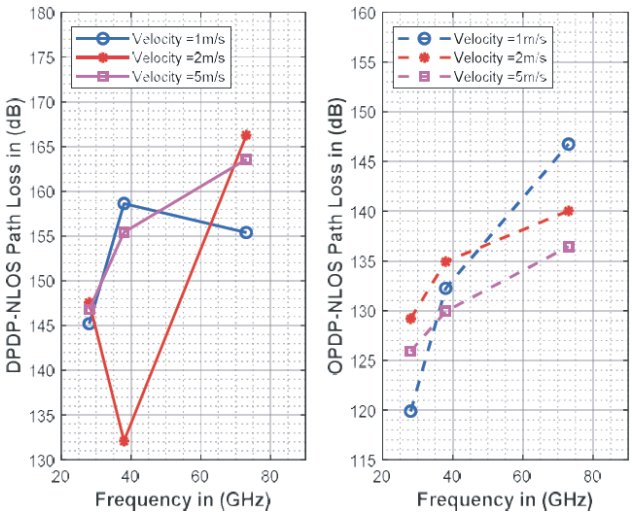

Figure 19. Path loss for DPDP and OPDP NLOS on velocity of user terminal scenarios.

and 38 GHz channels.

Considering the previously mentioned channels, it was found that the 73 GHz channel was more influenced by the change in LOS/NLOS correlation distance, moving distance, especially in NLOS condition. Moreover, the results showed that the 38 GHz channel was more influenced by the change in velocity, and the user's track type, especially in LOS and DPDP NLOS condition. However, the 28 and 73 GHz channels are able to better support the velocity and track type effect.

Table 6. Directional and omnidirectional power delay statistics for user terminal velocity scenarios.

Freq Channel [GHz]	Scenario	Velocity (m/s)	Directional Power Delay Profile				Omnidirectional Power Delay Profile			
			RMS DS (ns)	Received Power [dBm]	PL [dB]	PLE	RMS DS (ns)	Received Power [dBm]	PL [dB]	PLE
28	LOS	1	8.7	−39.88	119.09	2.75	10.39	−72.33	102.33	1.95
	LOS	2	32.36	−54.34	133.56	3.38	27.96	−76.01	106.01	2
	LOS	5	21.78	−45.47	125.08	3.28	23.68	−72.11	102.11	2.1
	NLOS	1	18.55	−66	145.21	4.56	36.79	−89.89	119.89	3.18
	NLOS	2	56.36	−68.55	147.56	4.28	45.84	−99.19	129.19	3.36
	NLOS	5	41.69	−67.61	146.82	4.2	22.62	−95.92	125.92	3.17
38	LOS	1	22.33	−44.4	123.61	2.79	17.5	−74.74	104.74	1.91
	LOS	2	12.2	−49.63	128.84	3.26	16.78	−72.44	102.44	1.93
	LOS	5	0.07	−26.48	105.7	2.28	3.15	−65.92	95.92	1.75
	NLOS	1	58.72	−79.43	158.64	4.89	14.19	−102.25	132.25	3.53
	NLOS	2	46.55	−62.89	132.1	3.9	30.81	−104.93	134.93	3.54
	NLOS	5	59.46	−96.21	155.42	4.38	31.94	−99.93	129.93	3.15
73	LOS	1	19.9	−51.21	130.42	2.84	20.29	−81.21	111.21	1.94
	LOS	2	5.12	−50.85	130.56	3.43	15.65	−74.15	104.15	1.95
	LOS	5	19.45	−64.77	143.98	3.64	15.07	−81.01	111.01	2.02
	NLOS	1	31.01	−75.83	155.4	4.1	27.32	−116.75	146.75	3.7
	NLOS	2	126.2	−87.05	166.27	4.51	56.17	−110.04	140.04	3.28
	NLOS	5	102.38	−84.36	163.57	4.75	33.98	−106.45	136.45	3.3

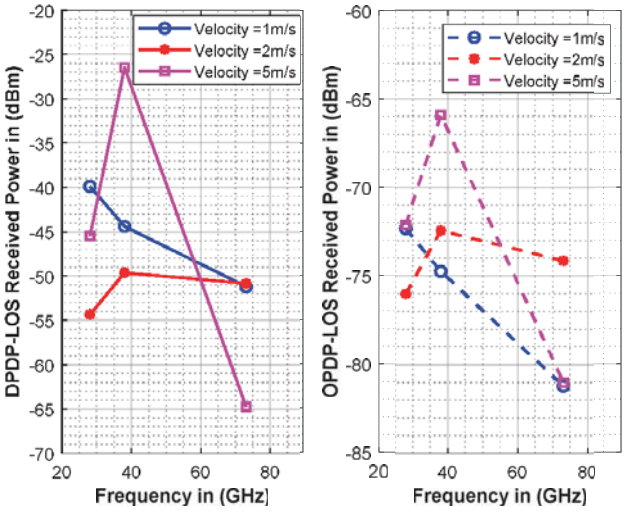

Figure 20. Received Power for DPDP and OPDP LOS on velocity of user terminal scenarios.

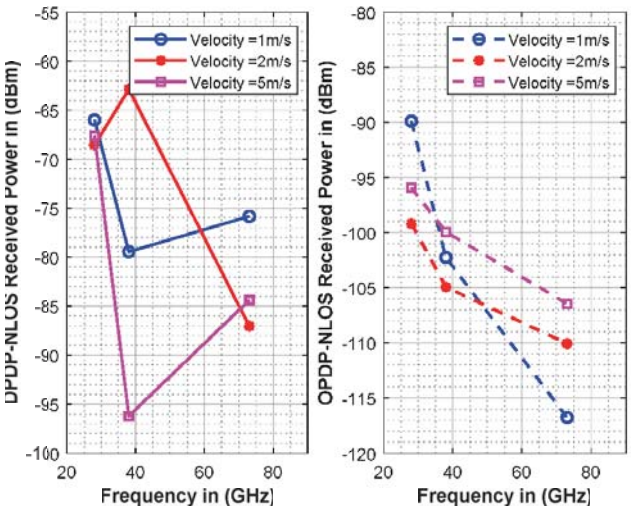

Figure 21. Received Power for DPDP and OPDP NLOS on velocity of user terminal scenarios.

Table 7. Spatial consistency parameters used in user track type scenarios.

Channel Parameters		**Antenna Parameters**	
RF Frequency	28/38/73 GHz	**TX/RX Array Type**	ULA/ULA
RF BW MHz	800	**Num TX/RX Elements**	1/1
Scenario	UMi	**TX/RX Antenna Elements Spacing**	$0.5\lambda/0.5\lambda$
Environment	LOS/NLOS	**TX Azimuth/Elevation HPBW**	$10°/10°$
T-R Separation (m)	100	**RX Azimuth/Elevation HPBW**	$10°/10°$
TX Power (dBm)	30	**Spatial consistency Parameters**	
Num RX	1	**Moving distance (m)**	40
Press (mbar)	1013	**Correlation distance LOS/NLOS (m)**	10
Hum %	50	**Update distance (m)**	1
Temp. C°	20	**Velocity (m/s)**	1
Pol	Co-Pol	**Track type**	Linear/Hexagonal
D Foliage (m)	0	**Moving direction (°)**	45°
Rain rate mm/hr	0		

Table 8. Directional and omnidirectional power delay statistics for user track type scenarios.

Freq Channel [GHz]	**Scenario**	**Track type**	**Directional Power Delay Profile**				**Omnidirectional Power Delay Profile**			
			RMS DS (ns)	**Received Power [dBm]**	**PL [dB]**	**PLE**	**RMS DS (ns)**	**Received Power [dBm]**	**PL [dB]**	**PLE**
28	LOS	Linear	32.33	−52.33	131.54	3.29	17.16	−76.34	106.34	2.11
	LOS	Hexagonal	35.18	−63.86	143.07	4.29	23.88	−78.49	108.49	2.47
	NLOS	Linear	38.57	−76.43	155.64	4.43	54.63	−94.26	124.26	2.95
	NLOS	Hexagonal	44.36	−69.76	148.97	4.57	24.53	−92.01	122.01	3.16
38	LOS	Linear	26.89	−34.33	113.54	2.66	22.76	−66	96	1.72
	LOS	Hexagonal	28.51	−55.25	134.47	3.5	12.43	−79.82	109.82	2.28
	NLOS	Linear	39.89	−72.58	151.79	4.13	35.44	−103.03	133.03	3.24
	NLOS	Hexagonal	127.53	−92.87	172.08	5.34	22.95	−103.83	133.83	3.45
73	LOS	Linear	25.53	−55.76	134.97	3.42	18.92	−76.02	106.02	1.9
	LOS	Hexagonal	26.24	−58.79	138	3.53	23.33	−74.07	104.07	1.77
	NLOS	Linear	185.18	−86.51	165.72	4.4	14.67	−109.66	139.66	3.26
	NLOS	Hexagonal	193.72	−91.25	170.46	5.24	17.36	−95.3	125.3	2.89

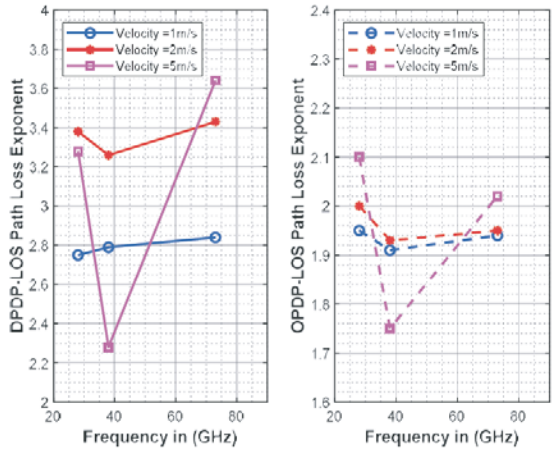

Figure 22. Path Loss Exponent for DPDP and OPDP LOS on velocity of user terminal scenarios.

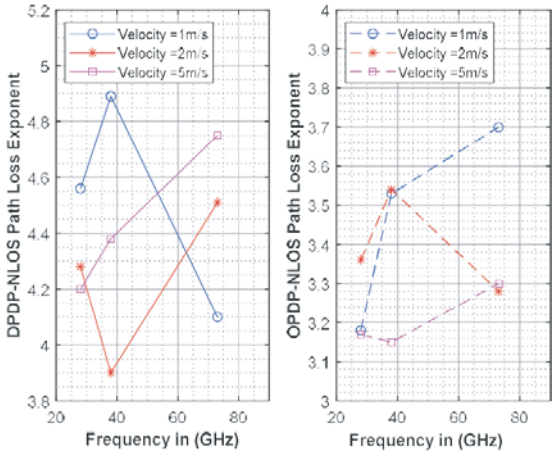

Figure 23. Path Loss Exponent for DPDP and OPDP NLOS on velocity of user terminal scenarios.

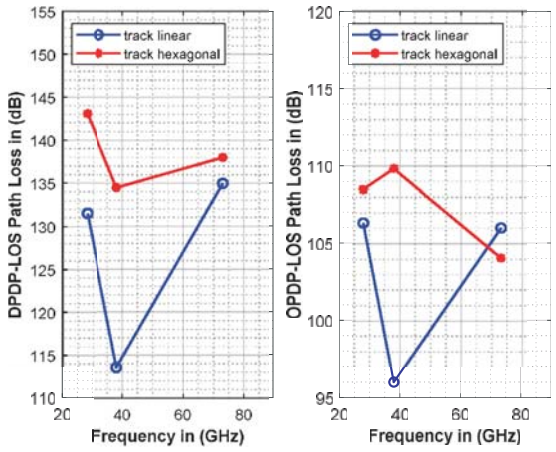

Figure 24. Path loss for DPDP and OPDP LOS on track type scenarios.

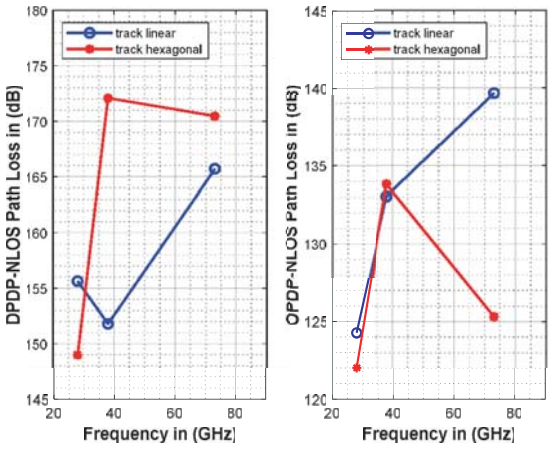

Figure 25. Path loss for DPDP and OPDP NLOS on track type scenarios.

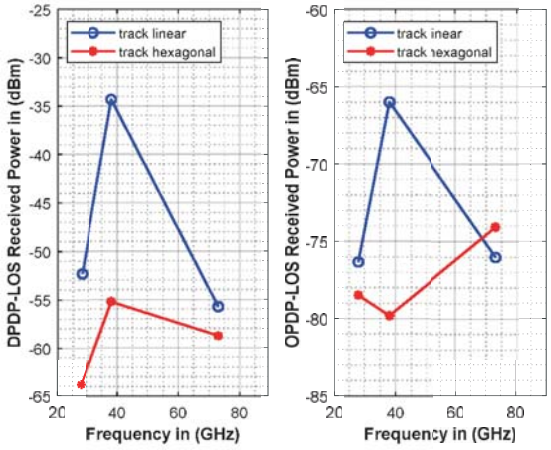

Figure 26. Received Power for DPDP and OPDP LOS on track type scenarios.

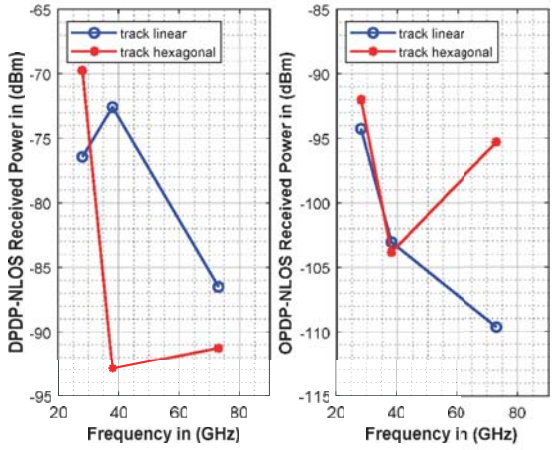

Figure 27. Received Power for DPDP and OPDP NLOS on track type scenarios.

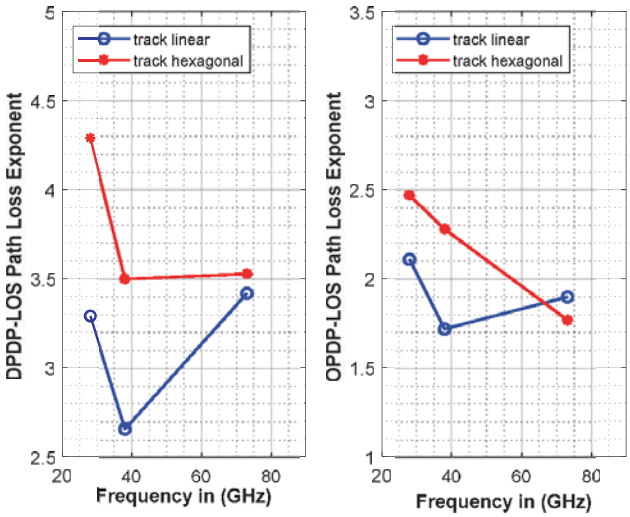

Figure 28. Path Loss Exponent for DPDP and OPDP LOS on track type scenarios.

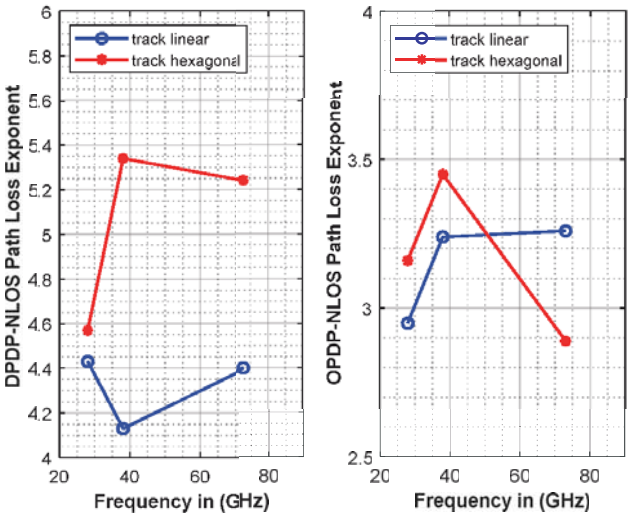

Figure 29. Path Loss Exponent for DPDP and OPDP NLOS on track type scenarios.

5. CONCLUSION

This paper statistically modeled the 28, 38, and 73 GHz millimeter wave bands intended to be employed by the 5G network considering spatial consistency scenarios: LOS/NLOS correlation distance, travel distance, user speed, user track type, for 5G UMi in LOS and NLOS scenarios. Besides, an extensive simulation was performed using the CI model adopted by the NYUSIM to analyze the impact of different spatial consistency parameters on the statistical characteristics of the channel such as path loss, received power, path loss exponent for directional power delay profile and omnidirectional power delay profile. The results showed that the performance of mmWave channels can be influenced by changing the spatial consistency parameters. This spatial analysis would be useful for exposing and developing the measurable channel model for 5G millimeter-wave communications.

ACKNOWLEDGMENT

The authors would like to support from Directorate General for Scientific Research and Technological Development (DGRSDT), Ministry of Higher Education and Scientific Research, Algeria.

REFERENCES

1. Rappaport, T. S., Y. Xing, G. R. MacCartney, A. F. Molisch, E. Mellios, and J. Zhang, "Overview of millimeter wave communications for fifth-generation (5G) wireless networks — With a focus on propagation models," *IEEE Transactions on Antennas and Propagation*, Vol. 65, No. 12, 6213–6230, Dec. 2017.
2. Ju, S. and T. S. Rappaport, "Millimeter-wave extended NYUSIM channel model for spatial consistency," *2018 IEEE Global Communications Conference (GLOBECOM)*, 1–6, Abu Dhabi, UAE, Dec. 2018.
3. Ju, S., O. Kanhere, Y. Xing, and T. S. Rappaport, "A millimeter-wave channel simulator NYUSIM with spatial consistency and human blockage," *2019 IEEE Global Communications Conference (GLOBECOM)*, 1–6, Hawaii, USA, Dec. 2019.
4. Ju, S., Y. Xing, O. Kanhere, and T. S. Rappaport, "Millimeter wave and sub-terahertz spatial statistical channel model for an indoor office building," *IEEE Journal on Selected Areas in Communications, Special Issue on TeraHertz Communications and Networking*, 1–15, Second Quarter 2021.

5. Ju, S., Y. Xing, O. Kanhere, and T. S. Rappaport, "3-D statistical indoor channel model for millimeter-wave and sub-terahertz bands," *2020 IEEE Global Communications Conference (GLOBECOM)*, 1–7, Dec. 2020.
6. Zaman, K. and M. M. Mowla, "A millimeter wave channel modeling with spatial consistency in 5G systems," *2020 IEEE Region 10 Symposium (TENSYMP)*, 1584–1587, 2020.
7. Docomo, N. T. T., "5G channel model for bands up to 100 GHz," *Tech. Report*, Oct. 2016.
8. Peter, M., et al., "Measurement results and final mmMAGIC channel models," *Deliverable D2*, Vol. 2, 12, 2017.
9. METIS2020, "METIS channel model," *Tech. Report*, Deliverable D1.4 v3, Jul. 2015.
10. Maltsev, A., et al., "WP5: Propagation, antennas and multiantenna techniques — D5.1: Channel modeling and characterization," *Millim.-Wave Evol. Backhaul Access (MiWEBA)*, Jun. 2014.
11. 3GPP, "Technical specification group radio access network; study on channel model for frequencies from 0.5 to 100 GHz (Release 14)," 3rd Generation Partnership Project (3GPP), TR 38.901 V14.2.0, Sept. 2017.
12. Nuckols, J. E., "Implementation of geometrically based single-bounce models for simulation of angle-of-arrival of multipath delay components in the wireless channel simulation tools, SMRCIM and SIRCIM," *Virginia Tech Library, Master of Science*, 1999.
13. Rappaport, T. S., S. Y. Seidel, and K. Takamizawa, "Statistical channel impulse response models for factory and open plan building radio communicate system design," *IEEE Transactions on Communications*, Vol. 39, No. 5, 794–807, May 1991.
14. Karttunen, A., A. F. Molisch, S. Hur, J. Park, and C. J. Zhang, "Spatially consistent street-by-street path loss model for 28-GHz channels in micro cell urban environments," *IEEE Transactions on Wireless Communications*, Vol. 16, No. 11, 7538–7550, Nov. 2017.
15. Ademaj, F. and S. Schwarz, "Spatial consistency of multipath components in a typical urban scenario," *2019 13th European Conference on Antennas and Propagation (EuCAP)*, 1–5, 2019.
16. Ademaj, F., S. Schwarz, T. Berisha, and M. Rupp, "A spatial consistency model for geometry-based stochastic channels," *IEEE Access*, Vol. 7, 183414–183427, 2019.
17. Samimi, M. K. and T. S. Rappaport, "3-D millimeter-wave statistical channel model for 5G wireless system design," *IEEE Transactions on Microwave Theory and Techniques*, Vol. 64, No. 7, 2207–2225, Jul. 2016.
18. Ju, S. and T. S. Rappaport, "Simulating motion — Incorporating spatial consistency into NYUSIM channel model," *2018 IEEE 88th Vehicular Technology Conference (VTC-Fall)*, 1–6, 2018.
19. Kyosti, P., et al., "WINNER II channel models," *Tech. Report*, European Commission, IST-WINNER, D1.1.2 V1.2, Feb. 2008.
20. Wang, Y., Z. Shi, L. Huang, Z. Yu, and C. Cao, "An extension of spatial channel model with spatial consistency," *2016 IEEE 84th Vehicular Technology Conference (VTC-Fall)*, 1–5, 2016.